Supporting Information

The Influence of Water on the Performance of Organic Electrochemical Transistors

Achilleas Savva,[†] Camila Cendra,[‡] Andrea Giugni,[#] Bruno Torre,[#] Jokubas Surgailis,[†] David Ohayon,[†] Alexander Giovannitti,[§] Iain McCulloch, [§,‖] Enzo Di Fabrizio,[#] Alberto Salleo,[‡] Jonathan Rivnay[▽] and Sahika Inal[†]*

[†] Biological and Environmental Science and Engineering, King Abdullah University of Science and Technology (KAUST), Thuwal 23955-6900, Kingdom of Saudi Arabia

[‡] Department of Materials Science and Engineering, Stanford University, Stanford, California 94305, United States

[#] SMILEs laboratory, Physical Science and Engineering, KAUST, Thuwal 23955-6900, Kingdom of Saudi Arabia

[§] Department of Chemistry, Imperial College London, SW72AZ, UK

[‖] PSE, KAUST Solar Center (KSC), KAUST, Thuwal 23955-6900, Kingdom of Saudi Arabia

[▽] Department of Biomedical Engineering, Northwestern University, Evanston, Illinois, 60208, United States

*sahika.inal@kaust.edu.sa

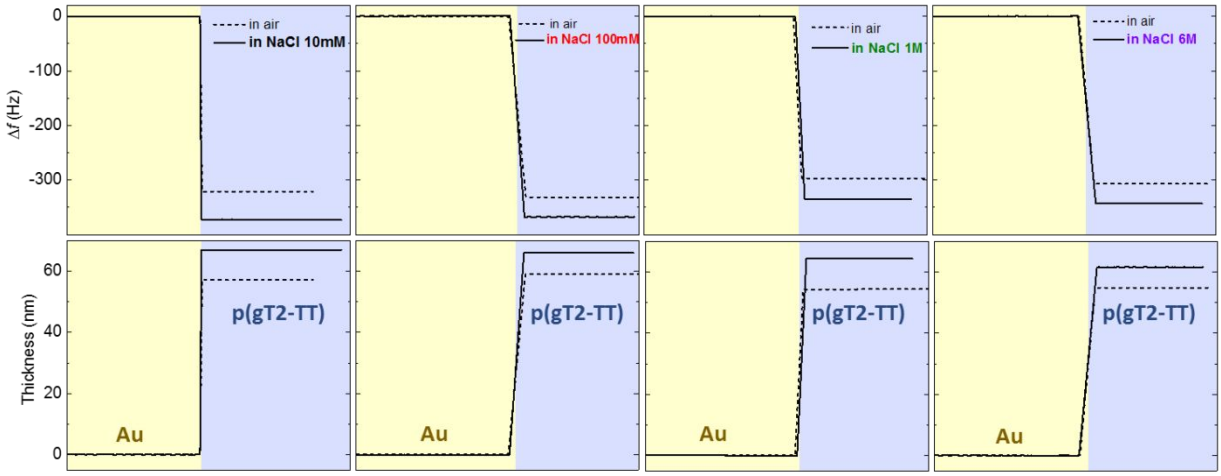

Figure S1: Frequency shifts (Δf) and the corresponding thicknesses of p(gT2-TT) films cast on Au coated sensors, recorded in air and when immersed in aqueous NaCl solutions of different concentrations. From left to right, the electrolyte is $NaCl_{(aq.)}$ 10 mM, 100 mM, 1 M and 6 M. Here, the 5th overtone for Δf is shown.

Table S1: Dry and wet thicknesses as well as swelling percentage calculated using the Sauerbrey equation for p(gT2-TT) films in different electrolytes.

NaCl concentration (M)	Dry thickness [nm]	Thickness in electrolyte [nm]	Swelling [%]
0.01	58	66	13
0.1	59	65	10
1	54	62	12
6	55	61	11

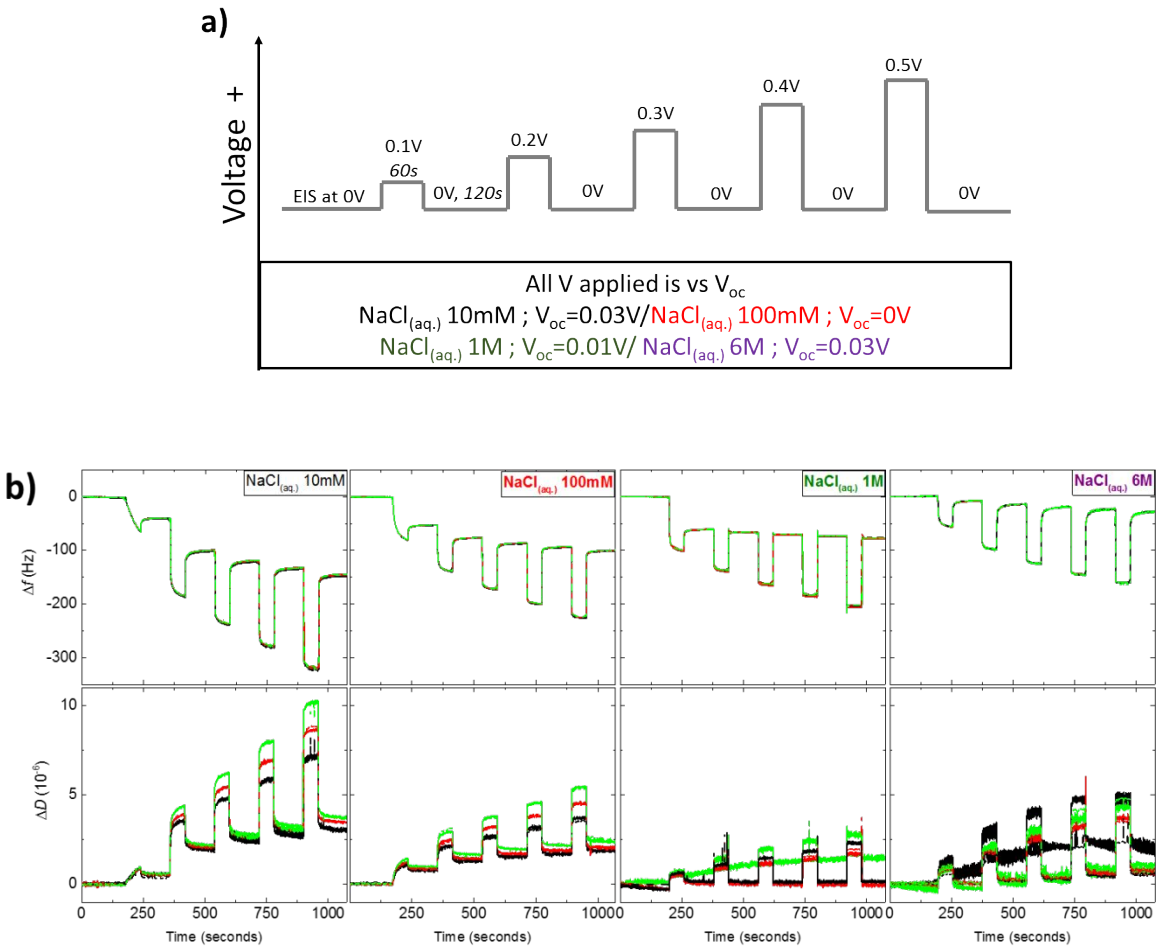

Figure S2: a) The potential routine followed during the EQCM-D measurements **b)** The EQCM-D frequency (Δf) and dissipation (ΔD) shifts recorded during biasing of the p(g2T-TT) film in four different electrolytes ($NaCl_{(aq.)}$, from left to right: 10 mM, 100 mM, 1 M, 6 M). The overtones shown and chosen for the analysis are the 5th, 7th and 9th; black, red and green lines, respectively.

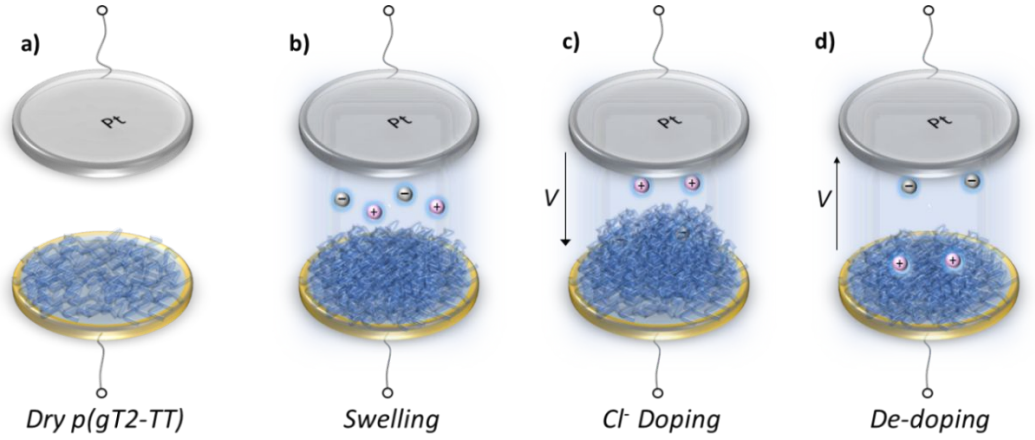

Figure S3: Schematic representation of p(g2T-TT)-NaCl system in the EQCM-D chamber during the course of the measurements: **a)** dry film, **b)** initial swelling (volumetric expansion) when the film is immersed in NaCl solution, **c)** further swelling caused by the injection of Cl^- anions under doping potentials, **d)** shrinkage of the film caused by the ejection Cl^- ions under de-doping potentials.

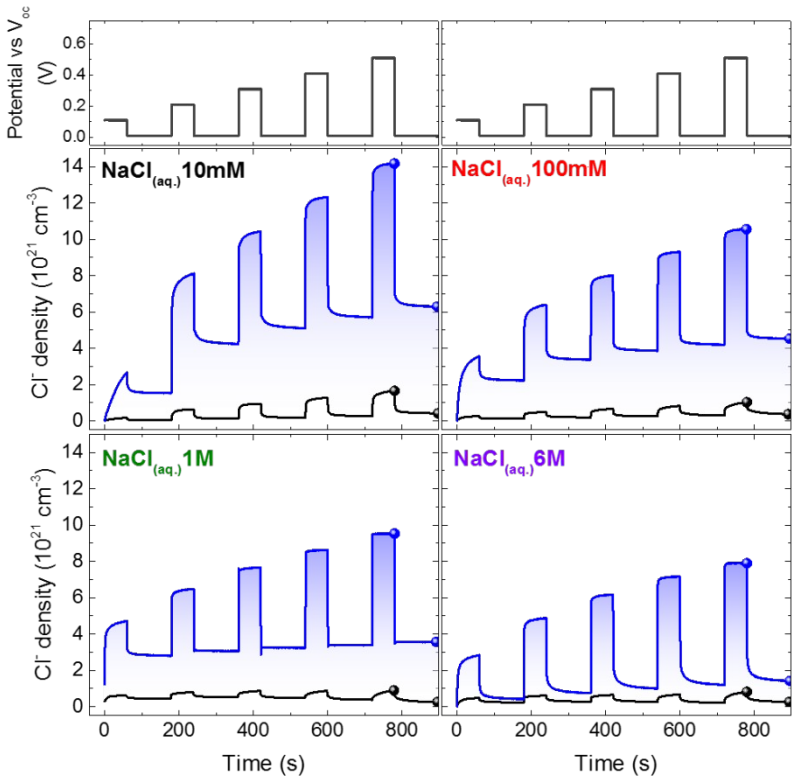

Figure S4: Real time monitoring of the number of the injected Cl^- ions, calculated from EQCM-D mass changes (blue lines) and from current *vs* time traces (black lines) during the evolution of the EQCM-D measurements in electrolytes of varying ion concentrations. The filled space between the blue and black curves represents water molecules incorporated into the films. The points marked on the curves are the data used to construct Figure 1c.

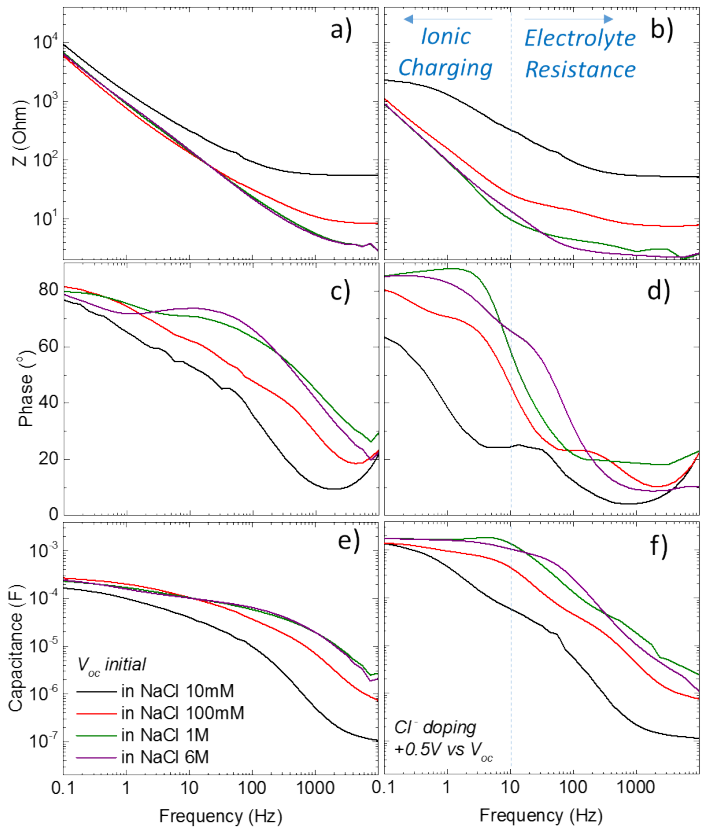

Figure S5: a-b) The magnitude, **c-d)** the phase of the impedance of p(g2T-TT) films recorded in four different electrolyte concentrations at $V = V_{OC} = 0$ V prior to biasing (left column) and at $V =$ +0.5 V vs V_{OC} (right column plots). **e)** and **f)** are the corresponding capacitance *vs* frequency plots.

Table S2: Lamellar and π-stacking spacings extracted from fitting the (200) and (010) peak, respectively, of the out-of-plane and in-plane lineouts shown in Figure S6 and Figure S7.

Bias condition	**Voltage step**	**$NaCl_{(aq.)}$ 10 mM**		**$NaCl_{(aq.)}$ 1 M**	
		$d_{(200)}$	**$d_{(010)}$**	**$d_{(200)}$**	**$d_{(010)}$**
Dry film	**1**	13.45	3.80	13.45	3.79
at 0V	**2**	13.59	3.74	13.46	3.78
at 0.5V (doping)	**3**	15.42	3.47	15.27	3.46
at 0V (after doping)	**4**	15.39	3.50	15.39	3.50

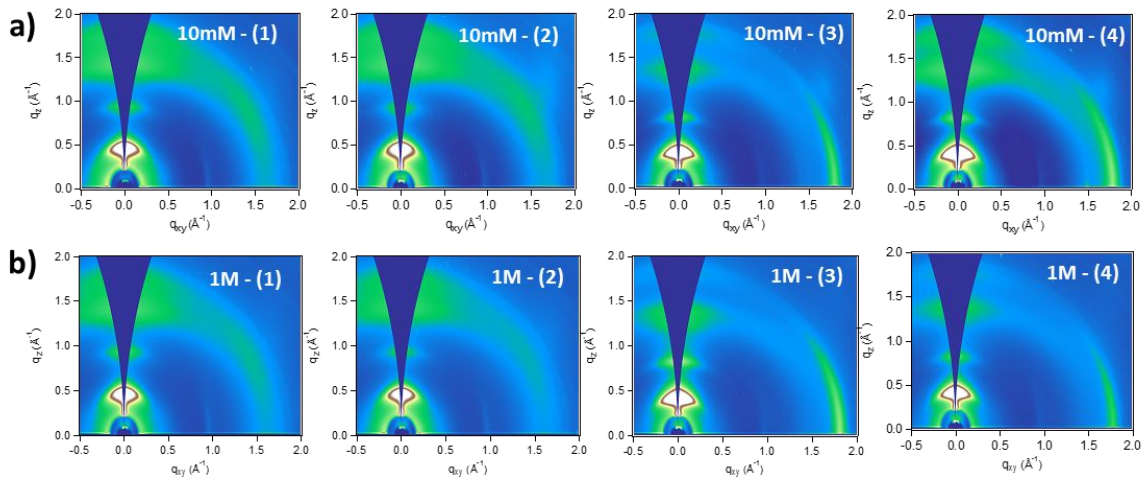

Figure S6: GIWAXS 2D patterns of p(gT2-TT) films electrochemically doped following the voltage procedure **a)** with $NaCl_{(aq.)}$ 10 mM and **b)** $NaCl_{(aq.)}$ 1 M.

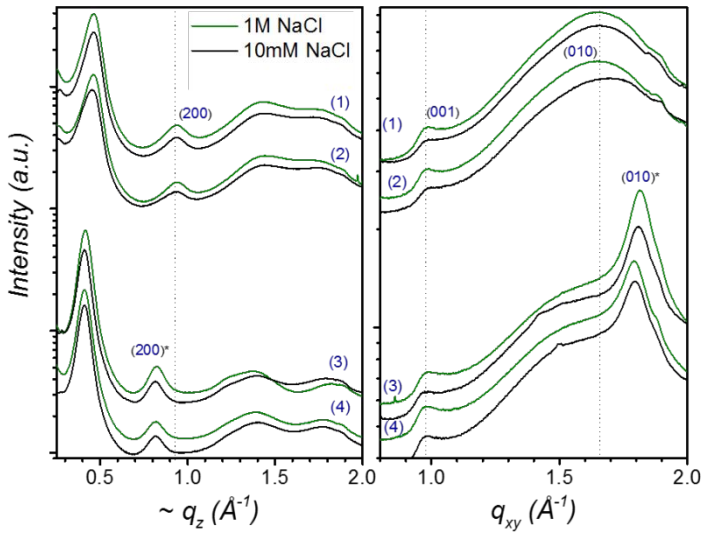

Figure S7: Out-of-plane ($\sim q_z$) and in-plane (q_{xy}) scattering lineouts for p(g2T-TT) films doped with $NaCl_{(aq.)}$ 10 mM and 1 M following the same doping proceudure as main figure 4. Dashed black lines correspond to center of the (200) and (010) scattering peaks in dry p(gT2-TT) for the out-of-plane and in-plane directions, respectively. Dotted black line is the backbone repeat (001).

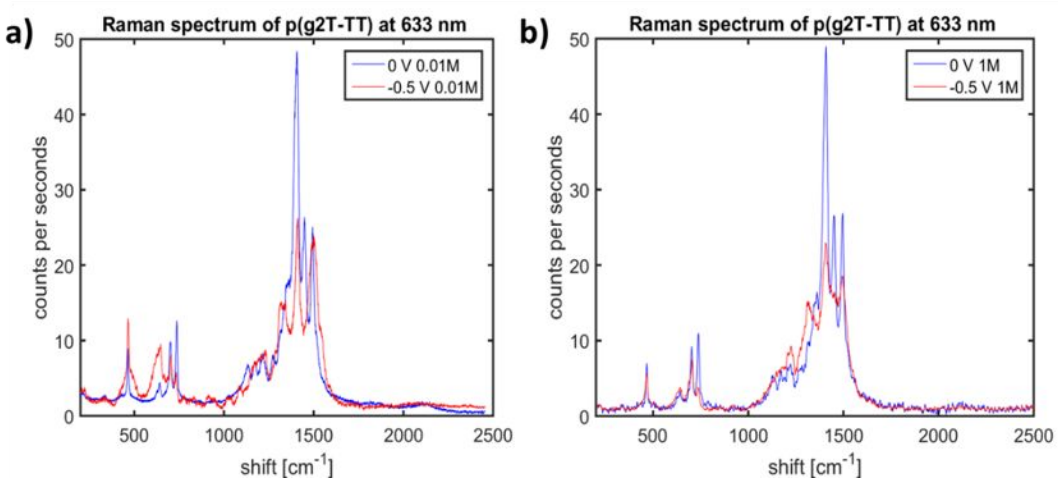

Figure S8: Raman intensity changes upon electrochemical doping with **a)** $NaCl_{(aq.)}$ 1 M and **b)** $NaCl_{(aq.)}$ 10 mM. The reduction is attributed to photon absorption changes upon doping and reduced molecular polarizability.

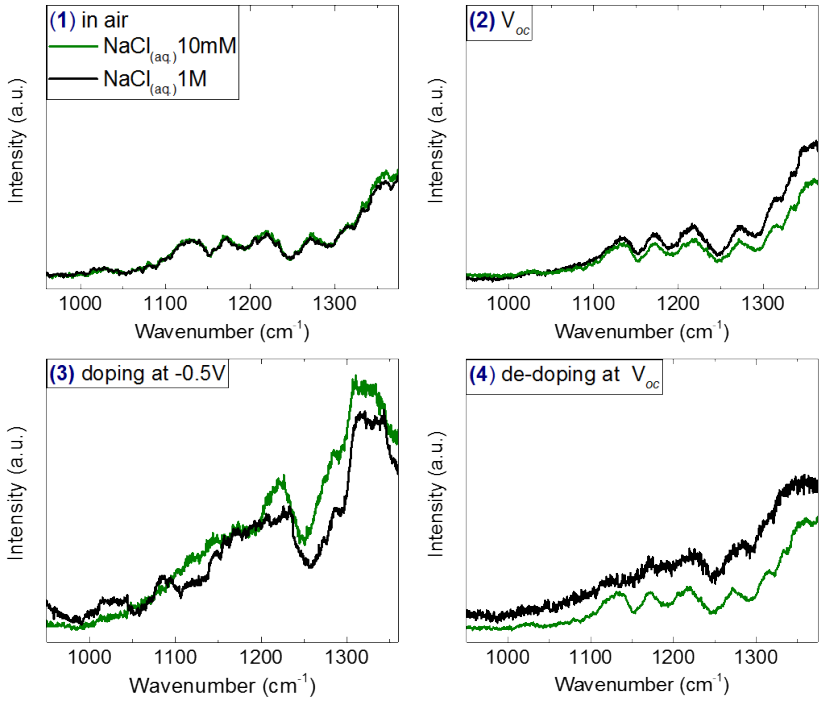

Figure S9: Raman spectra evolution (magnified at the region mainly associated with side chains) of the p(g2T-TT) films *during* doping in $NaCl_{(aq.)}$ 10 mM (black lines) and $NaCl_{(aq.)}$ 1 M (green

lines). The spectra were recorded when the film was dry, i.e., in air (1), immersed in electrolyte (2), doped at -0.5 V *vs* V_{OC} (3) and subsequently de-doped at V_{OC} (4).

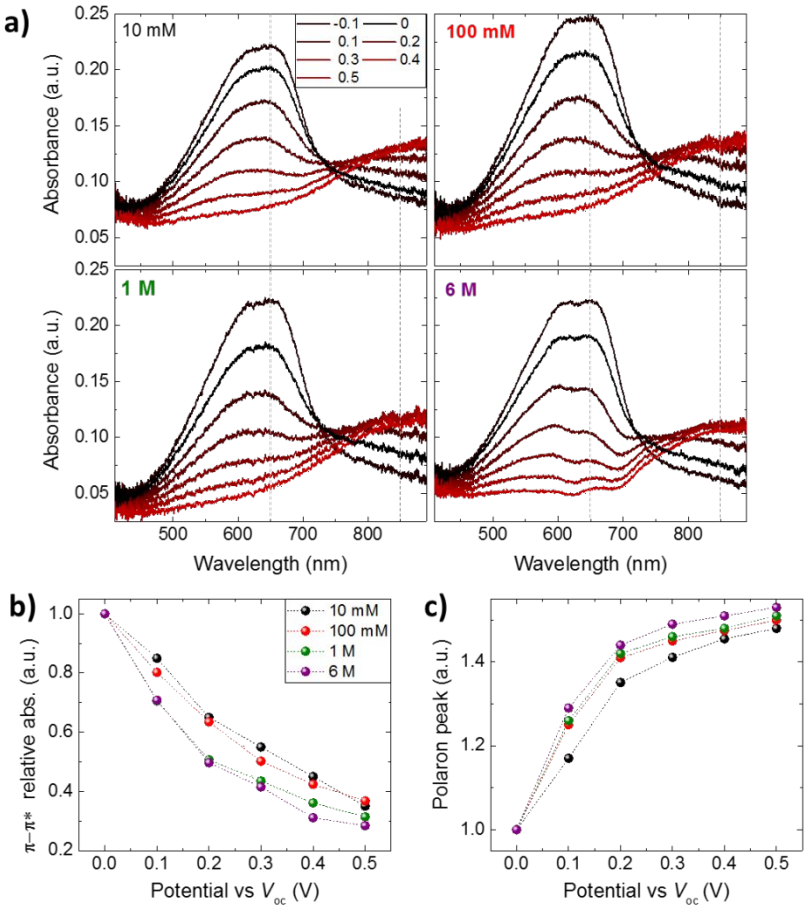

Figure S10: a) Absorbance spectra of four different p(g2T-TT) films exposed to doping potentials in $NaCl_{(aq.)}$ 10 mM, 100 mM, 1 M and 6 M. The changes in the spectra were monitored for the π-π* transition related absorption peak at 650 nm **b)** and for the polaron absorption **c)** as a function of potential applied *vs* V_{OC}.

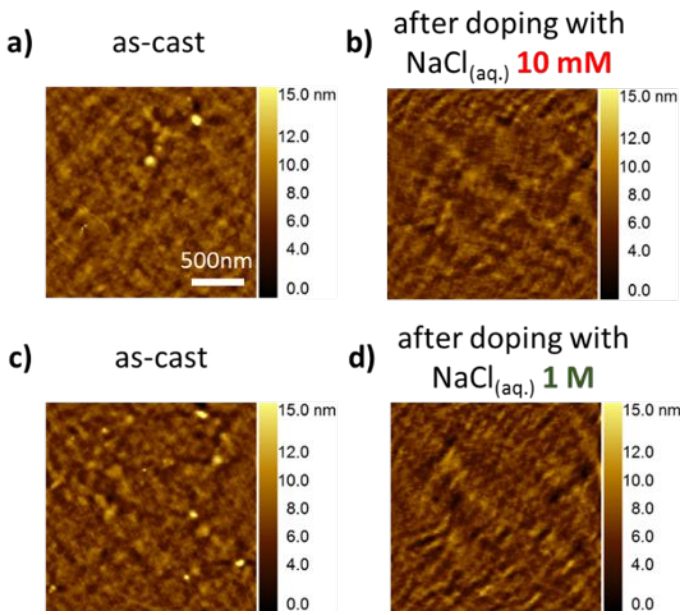

Figure S11: AFM images of **a-c)** as cast p(g2T-TT) films, **b)** after doping with $NaCl_{(aq.)}$ 10 mM and **d)** $NaCl_{(aq.)}$ 1 M .

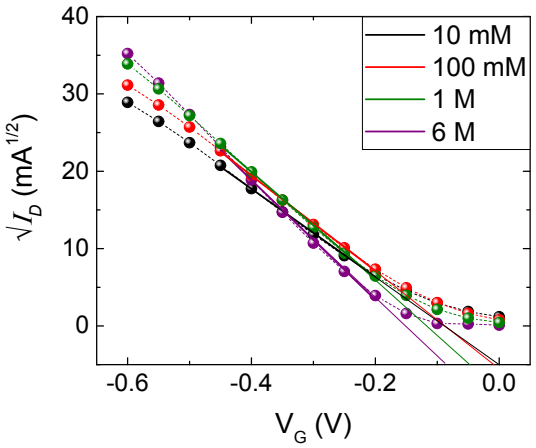

Figure S12: Square root of I_D versus the V_G of OECTs comprising of p(g2T-TT) in the channel and gated with an Ag/AgCl electrode immersed in $NaCl_{(aq.)}$ solutions with different ion concentrations. The points at which the solid lines intercept with the x-axis represent the corresponding threshold voltage.

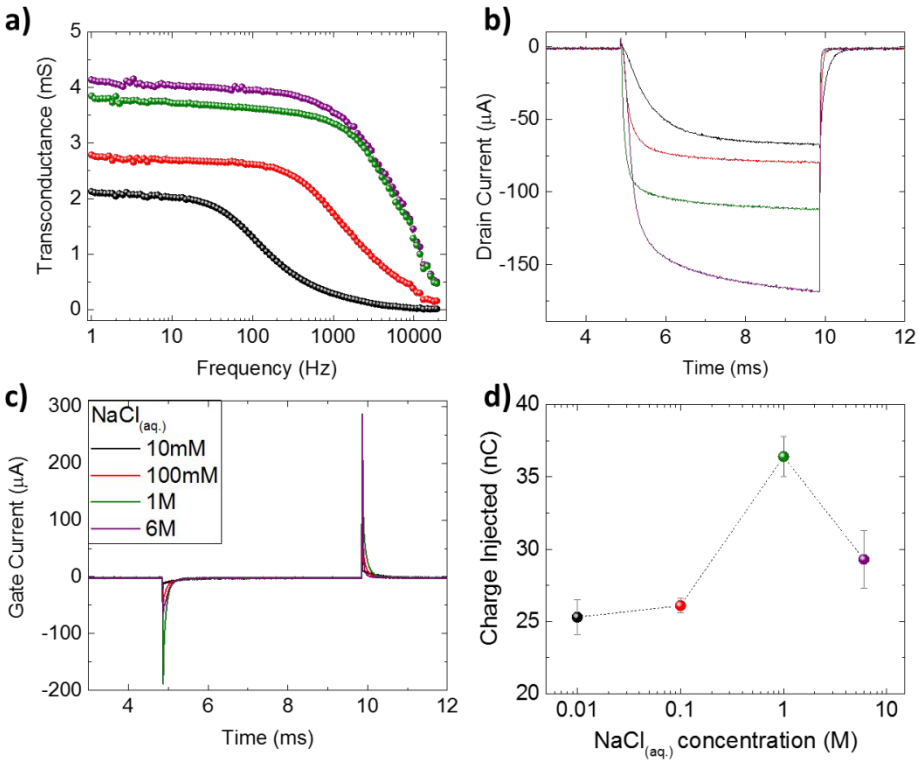

Figure S13: Transient measurements of the OECTs comprised of p(g2T-TT) channels gated with the four different $NaCl_{(aq.)}$ concentrations. **a)** Transconductance *vs* frequency plots for all the p(g2T-TT) based OECTs gated with different $NaCl_{(aq.)}$ concentrations. The devices were biased at a constant V_D and V_G of −0.5 V. Measurements were also performed at V_G varied between -0.1 V and -0.7 V and the results follow the trend shown here. **b)** Temporal response of the drain current and of **c)** the gate current, and **d)** the charge redistribution at the gate electrode *vs* $NaCl_{(aq.)}$ concentration when a 5 ms square voltage pulse (V_G = -0.5 V) is applied at the gate electrode for V_D = -0.5 V. The measurements are representative of one channel, while in d) we show results from 4 different channels.